Molecular Pharmacology Fast Forward. Published on December 28, 2009 as doi: 10.1124/mol.109.058115
This article has not been copyedited and formatted. The final version may differ from this version.

MOL #58115

Role for the RH Domain of GRK5 and 6 in β2-Adrenergic Receptor and Rhodopsin Phosphorylation

Faiza Baameur, Daniel H. Morgan, Hui Yao, Tuan M. Tran, Richard A. Hammitt, Subir Sabui, John S. McMurray, Olivier Lichtarge, and Richard B. Clark

Department of Integrative Biology and Pharmacology, University of Texas Health Science Center, Medical School, 6431 Fannin St, Houston, TX 77030, USA (FB, TMT, and RBC)

Department of Molecular and Human Genetics, Baylor College of Medicine, One Baylor Plaza, Houston, TX 77030, USA (DHM, HY, and OL)

Department of Experimental Therapeutics, The University of Texas M. D. Anderson Cancer Center, 1515 Holcombe Blvd, Houston, TX 77030, USA (RAH, SS, and JSMcM)

Molecular Pharmacology Fast Forward. Published on December 28, 2009 as DOI: 10.1124/mol.109.058115
This article has not been copyedited and formatted. The final version may differ from this version.

MOL #58115

GRK5 and 6 RH domain in GPCR phosphorylation

Richard B Clark

Department of Integrative Biology and Pharmacology, University of Texas Health Science Center, Medical School, 6431 Fannin St, Houston, TX 77030, USA

Tel: 713 500 7490

Fax: 713 500 7456

Email: richard.b.clark@uth.tmc.edu

Number of text pages: 20

Number of tables: 1

Number of figures: 9

Number of references: 41

Number of words in Abstract: 250

Number of words in Introduction: 799

Number of words in Discussion: 883

Abreviations

GPCR: G Protein-Coupled Receptor, GRK: G protein-Coupled Receptor Kinase, ET: Evolutionary Trace, RGS: Regulator of G protein Signaling, RH: RGS Homology, β2AR: Beta 2-Adrenergic Receptor, WT: Wild Type, ROS: Rod Outer Segment, Rho: Rhodopsin, ISO: Isoproterenol

Molecular Pharmacology Fast Forward. Published on December 28, 2009 as DOI: 10.1124/mol.109.058115
This article has not been copyedited and formatted. The final version may differ from this version.

Abstract: Phosphorylation of G Protein-Coupled Receptors (GPCRs) by GPCR Kinases (GRKs) is a major mechanism of desensitization of these receptors. GPCR activation of GRKs involves an allosteric site on GRKs distinct from the catalytic site. While recent studies have suggested an important role of the N- and C-termini and domains surrounding the kinase active site in allosteric activation, the nature of that site and the relative roles of the RH domain in particular remain unknown. Based on Evolutionary Trace (ET) analysis of both the RH and kinase domains of the GRK family, we identified an important cluster encompassing helices 3, 9 and 10 in the RH domain in addition to sites in the kinase domain. To define its function, a panel of GRK5 and 6 mutants was generated and screened by intact-cell assay of constitutive GRK phosphorylation of the β2-adrenergic receptor (β2AR), in vitro GRK phosphorylation of light-activated rhodopsin, and basal catalytic activity measured by tubulin phosphorylation and autophosphorylation. A number of double mutations within helices 3, 9, and 10 reduced phosphorylation of the β2AR and rhodopsin by 50-90% relative to WT GRK, as well as autophosphorylation and tubulin phosphorylation. Based on these results, helix 9 peptide mimetics were designed, and several were found to inhibit rhodopsin phosphorylation by GRK5 with an IC_{50} of ~ 30 μM. In summary our studies have uncovered previously unrecognized functionally important sites in the RH domain of GRK5 and 6, and identified a peptide inhibitor with potential for specific blockade of GRK-mediated phosphorylation of receptors.

Molecular Pharmacology Fast Forward. Published on December 28, 2009 as DOI: 10.1124/mol.109.058115
This article has not been copyedited and formatted. The final version may differ from this version.

In order to understand the mechanism underlying the activation of GRKs by the GPCRs, it is essential to identify functional sites in the GRKs involved in their activation. The serine/threonine GRK family includes seven members, GRK1-7, classified into three subfamilies on the basis of their sequence homology: the rhodopsin kinase subfamily (GRK1 and 7) activities of which are restricted to the visual system; the β-Adrenergic Receptor Kinase (βARK) subfamily (GRK2, and 3); and the GRK4 subfamily (GRK4-6) (Krupnick and Benovic, 1998; Pitcher et al., 1998). Crystal structures have been determined for GRK2 in complex with the βγ and Gαq subunits of G proteins (Lodowski et al., 2005; Lodowski et al., 2003; Lodowski et al., 2006; Tesmer et al., 2005), for GRK6 bound to AMPPNP (Lodowski et al., 2006), and recently for six crystal structures of rhodopsin kinase (Singh et al., 2008). These structures appear to be all in the inactive state. Thus neither the active-state conformation of GRKs nor how they interface with GPCRs is at present known.

Membrane localization and activation of GRKs are complex involving several domains within the kinase. It was shown that the GRK2 N-terminal fragment (residues 45-178) co-immunoprecipitated with metabotropic glutamate receptor 1 (Dhami et al., 2002), and that a single mutation in GRK2 (D527A) in the RH domain disrupted the GRK2-mGluR1 interaction (Dhami et al., 2004). Also, an early study showed that the binding of an antibody to the N-terminus of GRK1 blocked receptor phosphorylation (Palczewski et al., 1993). Moreover, in a yeast screen study, mutations within the GRK5 N-terminus were found to impair membrane localization and block rhodopsin phosphorylation (Noble et al., 2003). In a recent extension of these studies it was found that several N-terminal mutations of GRK2 (D3K, L4A and D10A) caused severe impairment of activity leading to the conclusion that the extreme N-terminus is involved in an intramolecular interaction that enhances GRK2 activity (Pao et al., 2009). Other

Molecular Pharmacology Fast Forward. Published on December 28, 2009 as DOI: 10.1124/mol.109.058115
This article has not been copyedited and formatted. The final version may differ from this version.

studies suggested a role for the C-terminus in the recognition of active GPCRs. A proline-rich motif within the C-terminus of GRK1, GRK2, and GRK5 mediates its association with light-activated rhodopsin (Gan et al., 2004). Also, it was shown that the C-terminus amphipathic helix of both GRK5 and 6 was required for plasma membrane localization and substrate (rhodopsin, tubulin) phosphorylation (Jiang et al., 2007; Thiyagarajan et al., 2004). It was also suggested that the dimer interface of GRK6 is a likely area of protein-protein interactions (Lodowski et al., 2006), and that residues 5-30 of the N-terminus and the C-terminal extension of the kinase domain proximal to the hinge region are possible sites for allosteric receptor binding (Singh et al., 2008). Recently, it was found that mutations in the GRK2 kinase domain, notably V477D, impair its phosphorylation of rhodopsin and β2AR (Sterne-Marr et al., 2009). Also a number of mutations in the kinase small and large lobes of GRK1 (R191A/K, Y274A, V476A and V484A) were found to block rhodopsin phosphorylation (Huang et al., 2009), and it was proposed that a cooperative interaction between the N-terminus and the kinase domain was important for GPCR activation. In summary while much has been learned from these studies, at present there has been no direct demonstration that mutant GRKs are defective in binding to GPCRs. This reflects the many difficulties associated with developing assays in these systems that resolve the complexities and potential overlap of GRK domains responsible for membrane binding, GPCR binding, and the transition to the active state.

To address the mechanism of GRK activation, we sought first to identify evolutionarily important sites of the GRK family that may be involved directly or indirectly in GPCR activation by Evolutionary Trace (ET). Past studies have shown that functionally important residues in proteins can be identified computationally by ET based on how well their sequence variations correlate with evolutionary divergence patterns (Lichtarge et al., 1996; Mihalek et al., 2004).

Molecular Pharmacology Fast Forward. Published on December 28, 2009 as DOI: 10.1124/mol.109.058115
This article has not been copyedited and formatted. The final version may differ from this version.

Using ET analysis, we found a number of statistically significant clusters in both the RH and kinase domains that suggest evolutionarily important regions specific to the GRK subfamily relative to the RGS proteins and serine/threonine protein kinase superfamilies respectively. We focused the present study on the RH terminal subdomain cluster involving helices 3 and 9, helix 10 proximal to the hinge region between RH and kinase domains, and the N-terminus. Our mutagenesis and functional studies were performed on GRK5 and 6, since our previous work and that of others demonstrated an important role for these GRKs in β2AR GRK site phosphorylation and desensitization (Shenoy et al., 2006; Tran et al., 2007; Violin et al., 2006; Wang et al., 2008).

Our findings demonstrate the importance of sites in helices 3, 9 and 10 in the RH domain in GPCR phosphorylation, and suggest they play a key role in supporting the conformational shift of the GRKs to the activate state.

Molecular Pharmacology Fast Forward. Published on December 28, 2009 as DOI: 10.1124/mol.109.058115
This article has not been copyedited and formatted. The final version may differ from this version.

Materials and Methods

Human Embryonic Kidney (HEK293) cells were purchased from the American Type Culture Collection (Manassas, VA). Cell culture reagents are from Mediatech (Herdon, VA). Lipofectamine 2000, and TOP 10 competent cells are from Invitrogen (Carlsbad, CA). Peptide N-glycosidase F (PNGaseF) was from New England Biolabs (Beverly, MA). Polyclonal primary antibodies to pS-(355,356) C-Tail of the β_2AR, and to GRK2, GRK5, and GRK6 are from Santa Cruz Biotechnology (Santa Cruz, CA). The polyclonal anti-c-myc antibody was purchased from Biovest International Inc./NCCC (Minneapolis, MN). N-terminal 6 His-tagged, recombinant, full length, human GRK5 was purchased from Millipore (Dundee, UK). The HRP-conjugated secondary antibody was from BioRad. Enhanced chemiluminescence SuperSignal reagent was purchased from Thermo Scientific (Rockford, IL), and blue X-ray film was from Phenix (Candler, NC). QuickChange Site-Directed Mutagenesis Kit was from Stratagene (La Jolla, CA). SP-Sepharose Fast Flow was purchased from GE Healthcare (Piscataway, NJ). Purified tubulin from bovine brain was purchased from Cytoskeleton (Denver, CO). Peptides 1-5 were purchased from Genemed Synthesis, Inc. (San Antonio, TX).

Cell culture. HEK293 cells stably overexpressing FLAG-tagged wild type (WT) β2AR (WT-β2AR) at 2-4 pmol/mg membrane were grown in 5% CO_2 at 37°C in Dulbecco's Modified Eagle's Medium (DMEM) containing 10% fetal bovine serum, 100 units/ml penicillin, 100 μg/ml streptomycin, and 200 μg/ml G418. When seeding cells for experiments dishes were coated with poly-L-lysine to aid attachment.

ET analysis. To rank the relative evolutionary importance of GRK sequence residues, we applied ET analysis (Lichtarge et al., 1996; Mihalek et al., 2004) separately to the RH and kinase domains of GRK. The RH trace was done in two ways, first as part of a global alignment of 270

Molecular Pharmacology Fast Forward. Published on December 28, 2009 as DOI: 10.1124/mol.109.058115
This article has not been copyedited and formatted. The final version may differ from this version.

aligned RGS proteins, and then including only 56 aligned sequences of GRKs (GRK1-7) from different species. Likewise, the kinase domain was traced first as part of a global alignment of 463 aligned Ser/Thr kinases, and then including only 50 GRK kinase domains. Residues in top 30^{th} percentile rank of importance produced clusters in the structure of GRK6 (PDB ID: 2ACX) as measured by a clustering z-score which indicates important sites for structure and function above a threshold of 2 (Mihalek et al., 2003). The GRK trace residues that overlapped those from the superfamily analyses of RGS and Ser/Thr kinase were considered global determinants not necessarily specific to GRK, but those that were traced uniquely among GRKs were considered specific to the latter (Lichtarge et al., 1997; Madabushi et al., 2004).

Mutagenesis of GRK5 and GRK6. The WT hGRK5 (NM_005308), hGRK6 (NM_001004106), and hGRK2 (NM_001619) cDNA plasmids were cloned into pcDNA3.1 +. The cDNA plasmid of membrane tethered GRK2-PP was also cloned into pcDNA3.1 +. It was constructed by adding a cDNA sequence to its C-terminus that encodes GFP[2] tag and an extra 17 amino acids k-ras sequence (KDGKKKKKKSKTKCVIM). This peptide contains a polybasic region and a prenylation site to ensure its plasma membrane localization. These plasmids were all gifts from Dr. Rasmus Jorgensen (7TM Pharma, and NovoNordisk, Denmark). All clones were verified by DNA sequencing. Using the QuickChange Site directed mutagenesis kit, single and double alanine substitutions of ET residues were generated. Direct DNA sequencing was performed on all plasmids to confirm the predicted sequence.

Intact-cell phosphorylation of the β2AR by WT or mutant GRK5/6. WT-β2AR cells growing in 35 mm plates were transiently transfected with 150 ng of WT or mutant GRK5 and 1.35 μg of empty vector (pcDNA3.1+) cDNA plasmids using Lipofectamine 2000 transfection reagent according to the manufacturer's instructions. Controls were transfected with empty vector only.

Molecular Pharmacology Fast Forward. Published on December 28, 2009 as DOI: 10.1124/mol.109.058115
This article has not been copyedited and formatted. The final version may differ from this version.

After 48 hours, cells were treated with the β2AR agonist isoproterenol (ISO) (100 nM), dissolved in the carrier, 0.1 mM ascorbate / 1 mM thiourea pH 7 (AT), or AT alone for 2 min. The β2ARs were then solubilized as previously described (Tran et al., 2004). Samples were resolved on 12% SDS-PAGE, transferred to nitrocellulose membrane and immunoblotted first with anti-pS-355,356 antibody, then stripped and reprobed with anti-C-Tail antibody, and stripped again and reprobed with the anti-GRK5/6 antibodies. Results were normalized first to the β2AR levels (anti-C-Tail) then to GRK5/6 levels (anti-GRK5/6).

Preparation of GRK5/6 from 21K membrane fractions. WT-β2AR cells were grown to ~ 60-70% confluence in 100 mm dishes. Cells were transfected with 8 μg of cDNA plasmid of either vector, WT or mutant GRK as described above. After 48 hours cells were washed with ice-cold PBS and scraped into 1 ml of ice-cold lysis buffer (20 mM Tris-HCl, pH 7.5, 1 mM EDTA, 1mM phenylmethylsulfonyl fluoride (PMSF), 20 μg/ml leupeptin, and 3 mM benzamidine), followed by homogenization. 21K membrane fractions were prepared as previously described (Tran et al., 2007), and for solubilization, suspended in 1 ml of lysis buffer supplemented with 50 mM NaCl, 0.02 % TritonX-100, 1 mM DTT (dithiothreitol). Samples were frozen at -80 °C and either used directly after dilution (see below), or partially purified on SP-Sepharose columns. The levels of GRKs were quantified by reference to standard curves generated with purified GST-GRKs as described (Tran et al., 2007).

Purification of GRK5 on SP-Sepharose. Cell lysates were diluted 10 times, in lysis buffer supplemented with 50 mM NaCl, 0.02 % TritonX-100, 1 mM DTT, and applied to an SP-Sepharose column. The resin (250 μl) was washed six times with 2 ml of lysis buffer before eluting GRK5 with 20 mM Tris-HCl, 1 mM EDTA, 450 mM NaCl, and 0.02% Triton X-100. The partially purified GRK5 was then diluted to a final salt concentration of 50 mM and assayed

Molecular Pharmacology Fast Forward. Published on December 28, 2009 as DOI: 10.1124/mol.109.058115
This article has not been copyedited and formatted. The final version may differ from this version.

for rhodopsin phosphorylation. Purification of GRK was assessed by westerns. No GRK other than GRK5 was detectable in this fraction, and the level of GRK5 was assessed by reference to standard curves generated with purified GST-GRK5 or 6His-GRK5 obtained from Millipore.

Phosphorylation of rhodopsin. Urea-stripped Rod Outer Segments (ROS) were prepared as described (Wilden and Kuhn, 1982). WT and mutant GRK, solubilized as described above from WT-β2AR 21K membrane fractions or following purification with SP-Sepharose chromatography, were diluted in lysis buffer (5-10 nM of GRK5 and GRK6) and incubated with 4 μM of rhodopsin in buffer B (20 mM Tris-HCl, pH 7.5, 1 mM EDTA, 10 mM $MgCl_2$, and 100 μM [γ^{32}P]ATP containing ~ 500 dpm / pmol) at 30°C in a final volume of 32 μl (Pronin and Benovic, 1997). Rhodopsin was activated by illumination (475 nm) for 30 sec (Ridge et al., 2006) just prior to incubation. Reactions were stopped after 10 min by addition of 4X SDS-sample buffer, and samples electrophoresed on a 12% SDS-PAGE. After transfer to nitrocellulose membranes, ^{32}P-labeled proteins were visualized by autoradiograms. With these levels of GRK5/6, rhodopsin phosphorylation was linear for 0 to 30 min. Controls including reactions with either GRK5, activated rhodopsin, or empty vector alone revealed no activity over background. ^{32}P-Rhodopsin bands were quantified by densitometry directly from autoradiograms, by using a Storm Molecular Dynamics Phosphorimager (GE Healthcare), and by direct counting of excised bands; comparable results were obtained from these measurements.

To examine peptide inhibition of GRK5 phosphorylation of light-activated rhodopsin (Rho*), 2 μl peptides (10, 30, and 100 μM) dissolved in DMSO were added to the reaction tube prior to assay for rhodopsin phosphorylation. SP-Sepharose-purified GRK5 (~ 6 nM) or purified 6His-GRK5 (4.6 nM) was incubated with Rho* (4 μM or as indicated) in the absence or presence

Molecular Pharmacology Fast Forward. Published on December 28, 2009 as DOI: 10.1124/mol.109.058115
This article has not been copyedited and formatted. The final version may differ from this version.

of peptides, in buffer B at 30°C, and processed as described above. Peptide concentrations were calculated based on absorbance at 280 nm.

Autophosphorylation of GRK5 and phosphorylation of Tubulin. C-myc-tagged WT and mutant GRK5 were expressed in HEK293 cells. 21K membrane fractions prepared as described above were solubilized and GRK5 immunoprecipitated (IP) by incubating with anti-c-myc antibody (1 µg / 400 µl sample for 1 hour at 4 ºC) followed by addition of 40 µl of a 50 % slurry of protein A-Sepharose and further incubation for one hour. The IP complex was collected and washed three times with 1 ml of 20 mM Hepes, pH 8.0, 500 mM NaCl, and once with 1 ml 20 mM Hepes, pH 8.0. 40 µl of the final wash buffer was then added to the pellet and assayed for both autophosphorylation and tubulin phosphorylation.

Autophosphorylation. To assay autophosphorylation, 5 µl of 5X kinase buffer (100 mM Tris-HCl, pH 7.5, 5mM EDTA, 25 mM $MgCl_2$, and 100 µM [γ^{32}P]ATP containing ~ 5000 dpm / pmol) was added to tubes containing 20 µl of myc-immunoprecipitated GRK5. Samples were incubated for 1 hour at 30 ºC and stopped by addition of 5X SDS-sample buffer. After gel electrophoresis and transfer to nitrocellulose membranes, ^{32}P-labeled GRK5 was visualized by autoradiography and normalized to GRK5 levels quantitated by westerns.

Tubulin. Tubulin phosphorylation was assayed as described above for autophosphorylation except for the addition of 500 nM tubulin to the reaction. ^{32}P incorporation into tubulin was measured and results normalized to GRK5 levels.

Computational design of peptide mimetics of Helix 9. The GRK5 native helix 9 (FFDRFLQWKWLE) is predicted by AGADIR (Munoz and Serrano, 1994) to have less than 5% helical propensity when it is in solution as a monomer (the top-ranked ET residues are underlined). This suggests that this fragment by itself may not fold into the appropriate

Molecular Pharmacology Fast Forward. Published on December 28, 2009 as DOI: 10.1124/mol.109.058115
This article has not been copyedited and formatted. The final version may differ from this version.

biologically relevant helix, so that it will be less active alone than when it is part of the whole structure. As an alternative, we sought to generate peptides that were more likely to natively fold into helices, but which also preserved the key residues that ET predicted should be important to function. A Peptide Builder algorithm was created to design three such helical peptides. For example, in the sequence x-x-x-F166-x-x-R169-x-x-Q172-W173-x-x-L176-x which shows the ET residues and the remaining free 'x' residues, residues 'x' were replaced over 500 iterations under the condition that a replacement was accepted only if helicity increased, or until a helicity of 85% helicity was reached. Peptide Builder generated a list of peptides which could be ranked by predicted helicity, hydrophobicity or charge. From this list three peptides (1, 2, and 3) were selected as shown in Table 1.

Synthesis of chemically modified peptides. The following method was used to generate GRK5 helix 9 peptides that were chemically modified to create side chain to side chain bridges to induce helical constraints as shown in Table 1 (peptides 7 and 8). Peptides 6, 7, and 8 were acetylated on the N-terminus and were synthesized as C-terminal amides. Polydimethylacrylamide-based PL-DMA resin (Varian, Inc) was treated overnight with neat ethylenediamine as described in Arshady et al. (Arshady et al., 1981). After thoroughly washing the resin with DMF/CH_2Cl_2, Fmoc-Rink amide linker was added in three-fold excess, as calculated from the nominal loading of 1 mmol/g. Coupling was mediated with 3-fold excesses of PyBOP, HOBt, and a 6-fold excess of DIEA. On completion of the coupling as judged by negative ninhydrin tests, the resin was drained, washed with DMF/CH_2Cl_2 and CH_2Cl_2 then dried under vacuum and stored. By weight gain the loading was 0.65 mmol/g. Peptides 6, 7, and 8 were synthesized in parallel on aliquots of 0.20 g of this resin (0.65 mmol/g, 0.13 mmol) on an AAPPTEC 348 multiple synthesizer employing a 16-well reactor block. Fmoc-amino acids were

Molecular Pharmacology Fast Forward. Published on December 28, 2009 as DOI: 10.1124/mol.109.058115
This article has not been copyedited and formatted. The final version may differ from this version.

added in 6-fold excess and coupling was mediated by DIPCDI/HOBt in 7 ml of DMF/CH_2Cl_2 (1:1). Note that Met165 was replaced by Nle to avoid oxidation of the sulfur group. Resins were washed 5× with 7 ml of DMF/CH_2Cl_2 (1:1) after coupling and deprotection steps. Fmoc deprotection was mediated by treatment of the resins for 5 and 15 minutes with 7 ml of 20% piperidine in DMF. For peptide 7, Fmoc-Glu(OPip)-OH was used at position 170 and Fmoc-Lys(Mtt)-OH was used at position 174. For Peptide 8, Fmoc-Glu(OPip)-OH was used at position 167 and Fmoc-Lys(Mtt)-OH was used at position 171. Peptides were acetylated at their N-termini by addition of acetic anhydride on the automated synthesizer. On completion of the amino acid chains, these two resins were treated with 1% trifluoroacetic acid (TFA) in CH_2Cl_2 (5×7 ml, 5 min each). After washing, cyclization was achieved by treatment of the resins with 3 equivalents each of diisopropylcarbodiimide and 1-hydroxybenzotriazole for 20 hr. All three peptides were cleaved from their resins with TFA:triethylsilane:H_2O (95:2.5:2.5) (Pearson et al., 1989) for 2 hr, the volumes were reduced, the products were precipitated in Et_2O and collected by centrifugation and dried. Peptides were purified by Sephadex G-25 chromatography (2.5×100 cm) in 0.1 M AcOH followed by reverse phase HPLC using gradients of acetonitrile in H_2O (both solvents containing 0.1% TFA). All peptides were greater than 95% pure and gave the correct mass by ESI TOF mass spectrometry.

Molecular Pharmacology Fast Forward. Published on December 28, 2009 as DOI: 10.1124/mol.109.058115
This article has not been copyedited and formatted. The final version may differ from this version.

Results

Evolutionary Trace Analysis of GRKs. To identify functionally important residues, we performed ET analysis of the GRK subfamily by first running two separate analyses for both the RH (Fig. 1A-D) and the kinase domains (Fig. 1E-G). The RGS proteins superfamily analysis included 270 protein sequences and the Ser/Thr kinase superfamily 463 sequences (Fig. 1B and 1F respectively). ET analysis was used to rank the evolutionary importance of each sequence residue over all of the proteins in the alignment. Thus, when applied to an entire family, the top-ranked residues which typically form clusters can be thought of as global determinants of function. In a second phase, we restricted ET analysis to the GRK subfamily only (56 sequences), thereby generating a different set of rank scores for each residue, such that the difference between the two traces allowed us to isolate GRK-specific determinants from global determinants. Our study focuses on both GRK5 and 6, and since these two kinases are > 70 % homologous in their amino acid sequence, and show near identical homology in the crucial region of the RH domain (Loudon and Benovic, 1994), we mapped our ET results onto the GRK6 structure (Lodowski et al., 2006) since no crystal structure has been published yet for GRK5.

For the RGS proteins superfamily, our analysis of the top 30% ranked ET residues showed a cluster centering on helices α4, α5 and α7 (Fig. 1B). A number of these residues in GRK2 helix 5 are known to form a binding interface with the Gαq subunit of the G protein both from mutagenesis and the crystal structure (R106, D110, L118, and Q133 (α6)) (Day et al., 2004; Sterne-Marr et al., 2003). In addition to this site, the GRK subfamily analysis revealed a separate cluster of important residues (Fig. 1C). Difference analysis (Fig. 1D) reveals a conserved cluster including helices α0, α1 α3, α9, α10 and α11, presumably domains functionally important in the

Molecular Pharmacology Fast Forward. Published on December 28, 2009 as DOI: 10.1124/mol.109.058115
This article has not been copyedited and formatted. The final version may differ from this version.

GRK subfamily. Results for the difference ET analysis of the kinase domain superfamily and GRK subfamily are shown in Fig. 1G. Although in the present study these residues were not further examined, ET revealed interesting features consistent with results from the mutagenesis studies outlined above (Huang et al., 2009; Sterne-Marr et al., 2009).

To enable a better visualization of the total trace results, analyses for both the RH and the kinase domains were combined and projected on the GRK6 structure (Lodowski et al., 2006) as shown in Fig. 2, and on a surface diagram (Fig. S2). The domains unique to the GRK subfamily for the RH domain (red) and the kinase domain (yellow) are contrasted with those residues shared by the GRK subfamily with the superfamilies (pink and orange respectively). Based on the evidence provided by the ET for the potential importance of helices α0, α3, α9, and α10, residues in these regions were mutated and analyzed for functional effects. Of note, part of this site is buried under the C-terminus; however, we reasoned that this site was still close enough to the surface to be accessible to GPCRs, and that the C-terminal tail as well as the N-terminus might possibly undergo conformational rearrangements that may expose it further.

Mutagenesis of top ranked residues in GRK5: Effects on constitutive phosphorylation of the β2AR. To test whether the RH domain sites identified by ET analysis are involved in activation of GRKs by GPCRs (the top-ranked red residues shown in Figs. 1D and 2), single and double mutations of a number of key trace residues in helices 3, 9, and 10 of GRK5 were generated by alanine substitution to avoid introducing any charged amino acids. Alanine mutations of these residues are justified since most do not exhibit an alanine in different GRKs, and if they do this is rare and in a distant branch. Constitutive GRK site phosphorylation was then used as a screen to assess WT and mutant GRK5 activity. We have shown an important role of GRK5 in phosphorylation of S(355,356) of the β2AR using both HEK293 and COS7 cells, and that

Molecular Pharmacology Fast Forward. Published on December 28, 2009 as DOI: 10.1124/mol.109.058115
This article has not been copyedited and formatted. The final version may differ from this version.

transient overexpression of GRK5 causes a strong constitutive phosphorylation of the β2AR in these cells unlike GRK2 (Tran et al., 2004; Tran et al., 2007). Choosing this approach to evaluate GRK mutants is based on considerable evidence that overexpression of the β2AR correlates with an increasing fraction of constitutively active receptor (R*) (Samama et al., 1993; Whaley et al., 1994). The 30-50 fold overexpression of GRKs leads to constitutive phosphorylation of the β2AR consistent with it reflecting ligand-induced phosphorylation. The advantage of this method stems from it allowing assessment of mutant activity in an intact cell setting.

To optimize the assay, we first determined the level of GRK plasmid to achieve approximately half the GRK site phosphorylation relative to 100 nM isoproterenol (ISO) stimulation. Cells were transfected with a range of cDNA plasmid levels, and a level of 150 ng / well (35 mm) was found to be optimal and was used in the constitutive assays of the mutants. A typical result demonstrating the constitutive phosphorylation of the β2AR by WT GRK2, 5 and 6, and membrane-tethered GRK2 (GRK2-PP) is shown in Fig. 3. Phosphorylation of the receptor was measured by western blotting with the anti-pS(355,356) antibody (Tran et al., 2004; Tran et al., 2007) followed by normalization to the level of receptor expressed (C-Tail antibody). It can be seen that GRK5 and 6 gave similar levels of constitutive phosphorylation of the β2AR. Consistent with previous results, GRK2 gave no response above controls, although when membrane-tethered, its activity approached that of GRK5 and 6.

The results of our screen for the single and double mutations of GRK5 in the constitutive assay are shown in Fig. 4. All results from westerns were normalized to the total receptor level (C-tail antibody), and to the level of GRK5 expressed. Single mutations of GRK5 were consistently as active as the WT GRK5, with the exception of R68A which showed double the activity relative to WT GRK5. In contrast a number of double alanine substitutions showed 50-

Molecular Pharmacology Fast Forward. Published on December 28, 2009 as DOI: 10.1124/mol.109.058115
This article has not been copyedited and formatted. The final version may differ from this version.

95% reduction in activity relative to WT GRK5; namely, mutants L66A-F166A, P61A-F166A, F166A-Q172A, F166A-W173A, Q172A-L176A, F166A-E514A, L66A-E514A, L66A-P37A, and L66A-H38A. These residues are within helices 3, 9, 10 and the N-terminus. Double mutants in helices 3 and 9 that showed the most dramatic reductions in GRK5 activity were on a face of the helices that would be exposed if helix 11 from the C-terminal domain is lifted away. Consistent with this the P61A-Q69A and F166A-Q69A mutants showed no significant effect on GRK5 activity, as the side chain of Q69 is directed away from the putative interaction surface. Since single substitutions of the residues failed to produce significant reductions in activity, it appeared that multiple hits were required to sufficiently affect GRK phosphorylation of the β2AR, at least without resorting to other, more deleterious substitutions than alanine.

Of importance, the level of expression of the defective GRK5 double mutants in WT-β2AR cells was not significantly altered (Fig. S1). We also found no effect of the double mutants on the distribution of GRK5 in the 21K membrane fractions relative to cytosol expression as compared to WT (Figs. 5 and S3). Further we have found that overexpression of key double mutants of GRK5 showing reduced constitutive activity, did not inhibit ISO stimulation of β2AR phosphorylation by endogenous GRKs, suggesting the lack of dominant negative activity (data not shown). These controls were important since some of the mutations are structurally close to the C-terminal amphipathic region (546-565) and N-terminal residues proposed to be the PIP_2 binding domain involved in membrane localization of GRK5 (Pronin et al., 1998) and a possible intramolecular interaction (Pao et al., 2009).

It is important to note that ideally one could assay the mutants in intact cells with agonist; however, at least in WT-β2AR cells, this must be measured in the background of rapid and

Molecular Pharmacology Fast Forward. Published on December 28, 2009 as DOI: 10.1124/mol.109.058115
This article has not been copyedited and formatted. The final version may differ from this version.

complete agonist-stimulated phosphorylation by endogenous GRKs that obscure any additional activity of transfected GRKs.

WT and mutant GRK5 activity in the phosphorylation of light- activated rhodopsin. To further monitor the activity of GRK5 mutants, we assessed their capacity to phosphorylate light-activated rhodopsin (Rho*) in an in vitro assay. While rhodopsin is not the natural substrate for GRK5 and 6, this assay has been demonstrated in numerous prior studies to be useful, and therefore provides further support for the effects of mutations on ligand-induced GPCR activation of phosphorylation. Initially we piloted this assay using WT and mutant GRK5 transiently expressed ~ 30-50 fold in WT-β2AR cells and partially purified by step elution from an SP-Sepharose column. However, although expression of the mutants is equivalent to that of the WT, most of the mutants showed low recovery in the purification process. Therefore we piloted an assay of the WT and mutant GRK5 by use of either direct solubilization of transfected cells or by generation of a 21K pellet followed by extraction of the GRK5 as outlined in Methods. Since identical activity of the WT GRK5 was obtained from either assay with no detectable background from endogenous GRKs, we used the solubilized 21K pellet fraction. Also, since GRK expression tended to be more variable in 100 mm dishes, we first monitored levels of expression by comparison to GST-tagged GRK5 as the standard as previously reported (Tran et al., 2007), and then adjusted levels such that approximately equivalent amounts of GRK constructs were used in the assay. The results shown in Fig. 5 demonstrate that the key GRK5 double mutants that were inactive in the constitutive phosphorylation assay displayed much reduced activity (92-98%) in their phosphorylation of Rho*, whereas the WT GRK5 as well as a double mutant (P61A-Q69A) with WT levels of activity in the constitutive β2AR phosphorylation showed robust activity. Importantly no activity from endogenous GRKs was

Molecular Pharmacology Fast Forward. Published on December 28, 2009 as DOI: 10.1124/mol.109.058115
This article has not been copyedited and formatted. The final version may differ from this version.

detected following transfection with the control pcDNA3.1 plasmid. Further, we detected no constitutive phosphorylation of dark-adapted rhodopsin in our assay either with increased Rho (as high as 32 μM) or up to 40 fold higher GRK5 levels (data not shown), consistent with 11 cis-retinal acting as an inverse agonist (Gether and Kobilka, 1998).

WT and mutant GRK5 autophosphorylation and tubulin phosphorylation. To further investigate GRK5 mutant effects on kinase catalytic activity, we monitored basal activity using two approaches: autophosphorylation and phosphorylation of tubulin, a non-receptor substrate for GRKs (Carman et al., 1998). Myc-tagged WT and several double mutants of GRK5 (F166A-P61A, F166A-L66A, F166A-W173A, Q172A-L176A) solubilized from 21K membrane fractions were immunoprecipitated and assayed for autophosphorylation. Mutants defective in constitutive β2AR and rhodopsin phosphorylation also showed reduced autophosphorylation (> 95% reduction relative to WT GRK5) (Fig. 6A). Immunoprecipitated GRK5 was also examined for phosphorylation of tubulin,. The defective mutants were also impaired in tubulin phosphorylation; activities were reduced to near control levels (Fig. 6B). The c-myc WT GRK5 consistently showed slower mobility on SDS gels relative to the mutants. This might be attributable to autophosphorylation since it is lacking in the mutants. Collectively these results demonstrate that the key GRK5 mutations inhibit basal kinase activity similar to their effect on receptor-stimulated activities.

Effects of WT and mutant GRK6 on constitutive β2AR and light-activated rhodopsin phosphorylation. Evolutionary Trace of the GRK family demonstrated that all of the GRKs shared a core of evolutionarily important residues in helices 3, 9, and 10; therefore the above observation in GRK5 should carry over to other members of the family. Since studies by us and others indicate that GRK6 plays a role in β2AR phosphorylation, we generated and tested several

Molecular Pharmacology Fast Forward. Published on December 28, 2009 as DOI: 10.1124/mol.109.058115
This article has not been copyedited and formatted. The final version may differ from this version.

single and double mutations of GRK6 that our studies with GRK5 showed to be important as well as some novel combinations. Their activity was determined in both the constitutive assay following transient expression in WT-β2AR cells, and the in vitro assay with rhodopsin using 21K membrane fractions expressing GRK6 constructs. Our findings shown in Fig. 7 demonstrate that key double mutations localized to helices 3 and 9 showed a 75-90% reduction in constitutive β2AR phosphorylation. Expression of most of the GRK6 mutants was reduced by ~ 20-40% relative to WT GRK6, and two mutants, Q172A and Q172A-L176A failed to be expressed and could not be assayed. Mutations that reduced GRK6 activity in the constitutive assay also showed > 95% reduced rhodopsin phosphorylation. Notably, mutant L66A-R69A, expression of which did not affect significantly β2AR constitutive phosphorylation, showed ~ 75% reduced rhodopsin phosphorylation (Fig. 8). These mutations also include combinations of residues in helices 3 and 9, or within helix 9 alone: Y166A-L66A, L66A-Q172A, Y166A-Q172A, Y166A-L176A, and Q172A-W173A. Thus while our mutagenesis of GRK6 was not as extensive as of GRK5, overall the results provide further support for the importance of these helices in GPCR activation of GRKs.

Peptide inhibition of GRK5 phosphorylation of light-activated rhodopsin. Based on our ET analysis and experimental observations of marked diminutions of select GRK5 and 6 double mutants of helices 3 and 9 on β2AR and rhodopsin phosphorylation, it seemed possible that a peptide mimetic of one of these helices that specifically conserved the key evolutionary residues might inhibit GRK activity. To address this question, we designed a series of peptide mimetics of helix 9, and tested whether they would show inhibition in the in vitro rhodopsin assay. Peptides shown in Table 1 were synthesized as follows: (i) the native sequence of GRK5 (peptides 5 and 6), and GRK6 (peptide 4); (ii) peptides designed by the Peptide Builder such that important ET

Molecular Pharmacology Fast Forward. Published on December 28, 2009 as DOI: 10.1124/mol.109.058115
This article has not been copyedited and formatted. The final version may differ from this version.

residues were kept unchanged while others were modified to optimize helicity and solubility (1, 1AA, 2, 2AA, and 3), and (iii) peptides chemically modified to lock helix 9 in an α helix (7 and 8). Peptide (100 μM) inhibition of partially purified GRK5 phosphorylation of rhodopsin was then examined as shown in Fig. 9A. Of the three Peptide Builder-designed peptides, 1 and 1AA showed ~ 73 and ~ 86% inhibition respectively. Peptides 2 and 3 had much reduced inhibitory activity. For the native helix 9 peptide of GRK5, peptide 5 (residues 166-177) or peptide 6 (164-178), in which M165 is replaced by Nle to avoid oxidation of the sulfur group, we found inhibitions of ~ 66 and ~ 82% respectively. The native GRK6 helix 9 (peptide 4) that differs in only two residues from that of GRK5 showed similar inhibition of rhodopsin phosphorylation as with GRK5, demonstrating that both the native peptides were active. For the chemically locked peptides 7 and 8, inhibitions were ~ 85 and ~ 51% respectively, indicating helicity is important. None of the peptides significantly inhibited GRK5 phosphorylation of Rho* at 10 μM; however, at 30 μM peptides 1AA, 4 and 6 showed significant inhibition (45, 40, and 63 % respectively) (Fig. 9B). These findings demonstrate that the native helix 9 peptides, locked peptides, and a peptide presenting the key residues on one face of the helix all inhibited phosphorylation. To further investigate the kinetics of peptide 6 inhibition, GRK5 activity was examined over varied concentrations of rhodopsin. The results shown in Fig. 9C suggest that the interaction of peptide with rhodopsin was complex, altering both the apparent Km as well as the Vmax, although the predominant effect was on the Vmax. We also examined the specificity of peptides 4 and 6 for GRK5 versus GRK6. As shown in Fig. 9D while both peptides inhibited GRK5 phosphorylation of rhodopsin, only peptide 4 (derived from GRK6) was effective against GRK6.

Molecular Pharmacology Fast Forward. Published on December 28, 2009 as DOI: 10.1124/mol.109.058115
This article has not been copyedited and formatted. The final version may differ from this version.

Discussion

The RH and kinase domain residues of GRKs evolve under unique evolutionary selection pressure in the GRK subfamily relative to that of the AGC kinase superfamily, and until recently, little was known about the role conserved RH domains might play in the concerted conformational change to the active state triggered by activated GPCRs. In the present work we initiated a difference ET study of the GRK subfamily relative to the RGS and kinase superfamilies based on the crystal structures of GRKs determined by Tesmer's group. This revealed a number of sequence positions that were uniquely evolutionarily important to the GRK subfamily. Focusing on a conserved cluster within helices 3, 9, and 10 within the RH domain we found numerous double mutations that significantly reduced GRK5 catalytic activity both in intact cell assays of β2AR phosphorylation and in cell-free assays of light-induced rhodopsin phosphorylation. Some of these mutants showed reduced basal activity as measured by both GRK5 autophosphorylation and tubulin phosphorylation. Several key combinations were in helix 9 alone. Other double mutations reducing activity involved either helices 3 and 10, (L66A-E514A), 9 and 10 (F166A-E514A), or loop α0-α1 in combination with helix 3 (L66A-H38A and L66A-P37A). Identical and closely related mutations of GRK6 also showed reduced activity in both the β2AR and the rhodopsin assays demonstrating that the effects of these mutations are not limited to GRK5, and could be observed with other subfamilies of the GRKs. Of importance our findings with both assays were generally in good agreement, although somewhat stronger inhibitions of our mutations were obtained in the rhodopsin assay.

Single mutations to alanine for all residues had no significant effect with the exception of R68A mutation that increases GRK5 constitutive activity on the β2AR and to a lesser extent rhodopsin phosphorylation. In the GRK6 crystal structure it appears that R68 likely forms a salt

bridge with D85 on helix 4 (Fig. S2A). D85 is also a highly conserved residue (from our ET analysis) suggesting that loss of R68-D85 interaction, may cause a conformational change that releases a constraint on the catalytic cleft facilitating its closure, hence an increase in activity. Recently, Liggett's group showed that a GRK5 polymorphism (Q41L) caused increased GRK5 activity (Wang et al., 2008). These findings collectively indicate that there may be a number of residues in GRK5 that when mutated facilitate activity.

Our findings with the functional assays suggested the possibility that a peptide mimetic could interfere with GPCR activation. To explore this, we synthesized a series of potential peptidomimetics of helix 9 and examined their inhibition of GRK phosphorylation of Rho*. We found that the native peptides from GRK5 (peptides 5 and 6) and GRK6 (peptide 4), as well as the Peptide Builder-designed peptide 1, inhibited GRK5 phosphorylation of Rho* (66-83%) at 100 μM. Peptide 6 showed half maximum effects at 30 μM and non-competitive inhibition from kinetic studies. The results with peptide 1 show proof of concept that the ET residues retained on one face of the helix are most critical. On the other hand the two other designed peptides (2 and 3) had considerably reduced inhibitory activity relative to peptide 1, perhaps reflecting loss of their ability to adopt a helical conformation caused by introduction of charged residues (Glu) that interfere with the binding of the peptide. The activity of these peptide mimetics appears to confirm and extend the ET-directed mutagenesis results, suggesting that the RH domain is important for activation. The complex kinetics of peptide inhibition and the lack of inhibition of GRK6 by the GRK5 peptide are most consistent with peptide binding to the GRK rather than rhodopsin. However since the binding site is unknown, disruption of the α3 – α9 interaction or other non-specific allosteric interactions remain plausible. Nonetheless, the peptides are of use as

Molecular Pharmacology Fast Forward. Published on December 28, 2009 as DOI: 10.1124/mol.109.058115
This article has not been copyedited and formatted. The final version may differ from this version.

lead agents for future development of a GRK inhibitor with higher potency and specificity that would be of potential use to the field.

As discussed above, other studies have established an important role of both the N-terminus and residues in the kinase domain of GRKs 1 and 2. It was proposed these sites may be involved either directly in the allosteric GPCR activation, or in intramolecular interactions of the N-terminus with residues surrounding the catalytic site that stabilize the active state (Huang et al., 2009; Pao et al., 2009; Sterne-Marr et al., 2009). Pao et al have also shown that a GRK2 peptide mimicking the N-terminal residues 1-14 non-competitively inhibited GRK2 phosphorylation of GPCRs (Pao et al., 2009), most consistent with interference with the proposed intramolecular mechanism. Complementing these findings our results suggest that the effects we report on RH domain mutations are most likely attributable to the positioning of the RH terminal subdomain in apposition to the small lobe of the kinase domain. That is, disruption of the RH sites (helices 3, 9 and 10) propagates an effect on the kinase domain, rather than by a direct interaction with GPCRs. Consistent with this interpretation, helices 3 and 9 in GRK structures lie buried in part under the C-terminal extension (helix 11) such that if this were a part of the allosteric interaction domain, this helix must be displaced to accommodate GPCRs. In summary this study provides new evidence for an important role of evolutionarily conserved sites in the RH domain that are required for GRK5 and 6 activity.

Molecular Pharmacology Fast Forward. Published on December 28, 2009 as DOI: 10.1124/mol.109.058115
This article has not been copyedited and formatted. The final version may differ from this version.

Acknowledgements

Thanks to Dr. Kevin Ridge from the Department of Biochemistry and Molecular Biology at UTHSC-Houston for providing ROS and expertise. Thanks to Dr. Richard Hammitt for the synthesis of peptides. Thanks to Chiyi Zhong of the Department of Experimental Diagnostic Imaging at MDACC for the mass spectrometry of peptides 6, 7, and 8. Thanks to Jackie Friedman for aiding our effort in so many ways in the Clark lab, and to Dr. Carmen Dessauer and Dr. Jeffrey Frost for their many useful comments and discussions.

References

Arshady R, Atherton E, Clive DLJ and Sheppard RC (1981) Peptide synthesis. Part 1. Preparation and use of polar supports based on poly(dimethylacrylamide). *J Chem Soc, Perkin Trans 1*:529-537.

Carman CV, Som T, Kim CM and Benovic JL (1998) Binding and phosphorylation of tubulin by G protein-coupled receptor kinases. *J Biol Chem* **273**(32):20308-20316.

Day PW, Tesmer JJ, Sterne-Marr R, Freeman LC, Benovic JL and Wedegaertner PB (2004) Characterization of the GRK2 binding site of Galphaq. *J Biol Chem* **279**(51):53643-53652.

Dhami GK, Anborgh PH, Dale LB, Sterne-Marr R and Ferguson SS (2002) Phosphorylation-independent regulation of metabotropic glutamate receptor signaling by G protein-coupled receptor kinase 2. *J Biol Chem* **277**(28):25266-25272.

Dhami GK, Dale LB, Anborgh PH, O'Connor-Halligan KE, Sterne-Marr R and Ferguson SS (2004) G Protein-coupled receptor kinase 2 regulator of G protein signaling homology domain binds to both metabotropic glutamate receptor 1a and Galphaq to attenuate signaling. *J Biol Chem* **279**(16):16614-16620.

Gan X, Ma Z, Deng N, Wang J, Ding J and Li L (2004) Involvement of the C-terminal proline-rich motif of G protein-coupled receptor kinases in recognition of activated rhodopsin. *J Biol Chem* **279**(48):49741-49746.

Gether U and Kobilka BK (1998) G protein-coupled receptors. II. Mechanism of agonist activation. *J Biol Chem* **273**(29):17979-17982.

Huang CC, Yoshino-Koh K and Tesmer JJ (2009) A surface of the kinase domain critical for the allosteric activation of G protein-coupled receptor kinases. *J Biol Chem*.

Jiang X, Benovic JL and Wedegaertner PB (2007) Plasma membrane and nuclear localization of G protein coupled receptor kinase 6A. *Mol Biol Cell* **18**(8):2960-2969.

Krupnick JG and Benovic JL (1998) The role of receptor kinases and arrestins in G protein-coupled receptor regulation. *Annu Rev Pharmacol Toxicol* **38**:289-319.

Lichtarge O, Bourne HR and Cohen FE (1996) An evolutionary trace method defines binding surfaces common to protein families. *J Mol Biol* **257**(2):342-358.

Lichtarge O, Yamamoto KR and Cohen FE (1997) Identification of functional surfaces of the zinc binding domains of intracellular receptors. *J Mol Biol* **274**(3):325-337.

Lodowski DT, Barnhill JF, Pyskadlo RM, Ghirlando R, Sterne-Marr R and Tesmer JJ (2005) The role of G beta gamma and domain interfaces in the activation of G protein-coupled receptor kinase 2. *Biochemistry* **44**(18):6958-6970.

Lodowski DT, Pitcher JA, Capel WD, Lefkowitz RJ and Tesmer JJ (2003) Keeping G proteins at bay: a complex between G protein-coupled receptor kinase 2 and Gbetagamma. *Science* **300**(5623):1256-1262.

Lodowski DT, Tesmer VM, Benovic JL and Tesmer JJ (2006) The structure of G protein-coupled receptor kinase (GRK)-6 defines a second lineage of GRKs. *J Biol Chem* **281**(24):16785-16793.

Loudon RP and Benovic JL (1994) Expression, purification, and characterization of the G protein-coupled receptor kinase GRK6. *J Biol Chem* **269**(36):22691-22697.

Madabushi S, Gross AK, Philippi A, Meng EC, Wensel TG and Lichtarge O (2004) Evolutionary trace of G protein-coupled receptors reveals clusters of residues that determine global and class-specific functions. *J Biol Chem* **279**(9):8126-8132.

Mihalek I, Res I and Lichtarge O (2004) A family of evolution-entropy hybrid methods for ranking protein residues by importance. *J Mol Biol* **336**(5):1265-1282.

Mihalek I, Res I, Yao H and Lichtarge O (2003) Combining inference from evolution and geometric probability in protein structure evaluation. *J Mol Biol* **331**(1):263-279.

Munoz V and Serrano L (1994) Intrinsic secondary structure propensities of the amino acids, using statistical phi-psi matrices: comparison with experimental scales. *Proteins* **20**(4):301-311.

Noble B, Kallal LA, Pausch MH and Benovic JL (2003) Development of a yeast bioassay to characterize G protein-coupled receptor kinases. Identification of an NH2-terminal region essential for receptor phosphorylation. *J Biol Chem* **278**(48):47466-47476.

Palczewski K, Buczylko J, Lebioda L, Crabb JW and Polans AS (1993) Identification of the N-terminal region in rhodopsin kinase involved in its interaction with rhodopsin. *J Biol Chem* **268**(8):6004-6013.

Pao CS, Barker BL and Benovic JL (2009) Role of the amino terminus of G protein-coupled receptor kinase 2 in receptor phosphorylation. *Biochemistry* **48**(30):7325-7333.

Pearson DA, Blanchette M, Baker ML and Guindon CA (1989) Trialkylsilanes as scavengers for the trifluoroacetic acid deblocking of protecting groups in peptide synthesis. *Tetrahedron Lett* **30**:2739-2742.

Pitcher JA, Freedman NJ and Lefkowitz RJ (1998) G protein-coupled receptor kinases. *Annu Rev Biochem* **67**:653-692.

Pronin AN and Benovic JL (1997) Regulation of the G protein-coupled receptor kinase GRK5 by protein kinase C. *J Biol Chem* **272**(6):3806-3812.

Pronin AN, Carman CV and Benovic JL (1998) Structure-function analysis of G protein-coupled receptor kinase-5. Role of the carboxyl terminus in kinase regulation. *J Biol Chem* **273**(47):31510-31518.

Ridge KD, Marino JP, Ngo T, Ramon E, Brabazon DM and Abdulaev NG (2006) NMR analysis of rhodopsin-transducin interactions. *Vision Res* **46**(27):4482-4492.

Samama P, Cotecchia S, Costa T and Lefkowitz RJ (1993) A mutation-induced activated state of the beta 2-adrenergic receptor. Extending the ternary complex model. *J Biol Chem* **268**(7):4625-4636.

Shenoy SK, Drake MT, Nelson CD, Houtz DA, Xiao K, Madabushi S, Reiter E, Premont RT, Lichtarge O and Lefkowitz RJ (2006) beta-arrestin-dependent, G protein-independent ERK1/2 activation by the beta2 adrenergic receptor. *J Biol Chem* **281**(2):1261-1273.

Singh P, Wang B, Maeda T, Palczewski K and Tesmer JJ (2008) Structures of rhodopsin kinase in different ligand states reveal key elements involved in G protein-coupled receptor kinase activation. *J Biol Chem* **283**(20):14053-14062.

Sterne-Marr R, Leahey PA, Bresee JE, Dickson HM, Ho W, Ragusa MJ, Donnelly RM, Amie SM, Krywy JA, Brookins-Danz ED, Orakwue SC, Carr MJ, Yoshino-Koh K, Li Q and Tesmer JJ (2009) GRK2 activation by receptors: role of the kinase large lobe and carboxyl-terminal tail. *Biochemistry* **48**(20):4285-4293.

Sterne-Marr R, Tesmer JJ, Day PW, Stracquatanio RP, Cilente JA, O'Connor KE, Pronin AN, Benovic JL and Wedegaertner PB (2003) G protein-coupled receptor Kinase 2/G alpha q/11 interaction. A novel surface on a regulator of G protein signaling homology domain for binding G alpha subunits. *J Biol Chem* **278**(8):6050-6058.

Tesmer VM, Kawano T, Shankaranarayanan A, Kozasa T and Tesmer JJ (2005) Snapshot of activated G proteins at the membrane: the Galphaq-GRK2-Gbetagamma complex. *Science* **310**(5754):1686-1690.

Thiyagarajan MM, Stracquatanio RP, Pronin AN, Evanko DS, Benovic JL and Wedegaertner PB (2004) A predicted amphipathic helix mediates plasma membrane localization of GRK5. *J Biol Chem* **279**(17):17989-17995.

Tran TM, Friedman J, Qunaibi E, Baameur F, Moore RH and Clark RB (2004) Characterization of agonist stimulation of cAMP-dependent protein kinase and G protein-coupled receptor kinase phosphorylation of the beta2-adrenergic receptor using phosphoserine-specific antibodies. *Mol Pharmacol* **65**(1):196-206.

Tran TM, Jorgensen R and Clark RB (2007) Phosphorylation of the beta2-adrenergic receptor in plasma membranes by intrinsic GRK5. *Biochemistry* **46**(50):14438-14449.

Violin JD, Ren XR and Lefkowitz RJ (2006) G-protein-coupled receptor kinase specificity for beta-arrestin recruitment to the beta2-adrenergic receptor revealed by fluorescence resonance energy transfer. *J Biol Chem* **281**(29):20577-20588.

Wang WC, Mihlbachler KA, Bleecker ER, Weiss ST and Liggett SB (2008) A polymorphism of G-protein coupled receptor kinase5 alters agonist-promoted desensitization of beta2-adrenergic receptors. *Pharmacogenet Genomics* **18**(8):729-732.

Whaley BS, Yuan N, Birnbaumer L, Clark RB and Barber R (1994) Differential expression of the beta-adrenergic receptor modifies agonist stimulation of adenylyl cyclase: a quantitative evaluation. *Mol Pharmacol* **45**(3):481-489.

Wilden U and Kuhn H (1982) Light-dependent phosphorylation of rhodopsin: number of phosphorylation sites. *Biochemistry* **21**(12):3014-3022.

Molecular Pharmacology Fast Forward. Published on December 28, 2009 as DOI: 10.1124/mol.109.058115
This article has not been copyedited and formatted. The final version may differ from this version.

Footnotes

a) This work was supported by the National Institute of Health [Grants GM031208, and GM066099, GM079656]; the March of Dimes [FY06-371]; the NCI [CA096652]; and the R. A. Welch Foundation Chemistry and Biology Collaborative grant from the John S. Dunn Gulf Coast Consortium for Chemical Genomics.

Molecular Pharmacology Fast Forward. Published on December 28, 2009 as DOI: 10.1124/mol.109.058115
This article has not been copyedited and formatted. The final version may differ from this version.

Legends for Figures

Figure 1. Difference ET analysis of the GRK RH and kinase domains. Evolutionary Trace shows strong clustering of the top 30% ranked residues mapped onto the GRK6 crystal structure. **A-D**: ET results mapping the important residues onto the RH domain of GRK6 with helix 11 and the kinase domain removed. **A**: Results of the GRK subfamily alone with a large cluster in terminal subdomain. **B**: ET results for the superfamily confirm global conservation in the bundle subdomain. **C**: The difference ET for the RH domain. **D**: Close up of conserved residues clustering in helices 3, 9, and 10 (red residues are subfamily-specific while pink residues are conserved in both the GRK/RGS superfamily). **E-G**: ET results for the kinase domain. **E**: Results of the GRK subfamily alone. **F: R**esults of the kinase superfamily; the top 30% ranked residues are shown in yellow for both the superfamily and subfamily. **G**: The Difference ET (yellow residues are subfamily specific while orange residues are conserved in both the superfamily and subfamily); the green molecule represents AMPPNP.

Figure 2. Evolutionary Trace analysis mapped onto GRK6. GRK6 x-ray structure PDB code 2ACX (Lodowski et al., 2006) is shown in cartoon using PyMol Molecular Graphics System. The structure shows the difference ET analysis of the RH domain (white and red), and the kinase domain (brown and yellow). Red and yellow colored residues represent the evolutionarily important residues unique to GRK subfamily.

Figure 3. β2AR constitutive phosphorylation by overexpression of GRKs. WT-β2AR cells were transiently transfected with either pcDNA 3.1+ (Control), GRK5, GRK2, GRK6, or GRK2-PP. After 48 hours, cells were treated with 100 nM ISO (filled bars) or the carrier AT (open bars) for 2 min, solubilized and processed for western blotting (Methods). The data were normalized to

Molecular Pharmacology Fast Forward. Published on December 28, 2009 as DOI: 10.1124/mol.109.058115
This article has not been copyedited and formatted. The final version may differ from this version.

the total receptor levels (α-C-Tail) and are means ± SEM of three experiments. Representative western blots are shown below the graph.

Figure 4. Effect of GRK5 mutations on constitutive β2AR GRK site phosphorylation. WT-β2AR cells were transiently transfected with WT or mutant GRK5. After 48 hours, cells were solubilized, lysates were run on SDS-PAGE, probed with anti-pS355, 356, and then stripped and reprobed with anti-C-Tail, and with anti-GRK5. The data were normalized to the total receptor levels and GRK5 levels. Several double mutations show significant decrease in GRK site phosphorylation (*** $p < 0.001$ or * $p < 0.05$ by One-way ANOVA). The data are means ± SEM of at least four experiments performed in duplicate. Representative Western blots are shown below the graph.

Figure 5. Effect of GRK5 mutations on Rho* phosphorylation. WT and mutant GRK5 were expressed in WT-β2AR cells, solubilized from the 21K membrane fractions (5-10 nM GRK5) and assayed as described in Methods. All the data shown are with light-activated rhodopsin with the exception of the WT GRK5 labeled dark. The control represents solubilized 21K membranes from cells transfected with only the empty vector (pcDNA3.1+). The reaction mix was run on SDS-PAGE and the autoradiogram was developed. Data show the percent activity of mutant GRK5 as compared to WT GRK5 and normalized to GRK5 expression levels. Quantitation was performed by use of Molecular Dynamics Storm Phosphorimager. The data are means ± SEM of at least three experiments performed in duplicate. One-Way ANOVA statistical analyses were determined (*** $p < 0.001$). Inset: Representative autoradiogram and GRK5 expression levels.

Figure 6. Effect of GRK5 mutations on autophosphorylation and tubulin phosphorylation. C-myc-tagged WT and mutant GRK5 were expressed in WT-β2AR cells, solubilized from the 21K membrane fractions, immunoprecipitated, and assayed for autophosphorylation **(A)**, and

Molecular Pharmacology Fast Forward. Published on December 28, 2009 as DOI: 10.1124/mol.109.058115
This article has not been copyedited and formatted. The final version may differ from this version.

tubulin phosphorylation **(B)** as described in Methods. Control represents activity from cells expressing the pCMV5-c-myc alone. Data show the percent activity of mutant GRK5 relative to WT and were normalized to GRK5 expression levels. The data are means ± SEM of at least three experiments. One-Way ANOVA statistical analyses were determined (*** $p < 0.001$, ** $p < 0.01$, and * $p < 0.05$). Representative autoradiograms and GRK5 expression levels are shown below each graph.

Figure 7. Effect of GRK6 mutations on constitutive β2AR GRK site phosphorylation. WT and mutant GRK6 were expressed in WT-β2AR cells and constitutive phosphorylation of the β2AR measured as described in the legend to Fig. 4. The data were normalized to the total receptor levels and GRK6 levels. The data are means ± SEM of four experiments performed in duplicate (*** $p < 0.001$ by One-Way ANOVA). Inset: Representative Western blots.

Figure 8. Effect of GRK6 mutations on Rho* phosphorylation. WT and mutant GRK6 were expressed in WT-β2AR cells, solubilized from the 21K membrane fractions (~ 5 nM GRK6) and assayed as described in the legend to Fig. 5. The percent activity of mutant GRK6 as compared to WT GRK6 was calculated, and normalized to GRK6 expression levels. The data are means ± SEM of three experiments performed in duplicate (*** $p < 0.001$ by One-Way ANOVA). Inset: Representative autoradiogram and GRK6 expression levels.

Figure 9. Peptide inhibition of GRK phosphorylation of Rho*. Illuminated rhodopsin was incubated with SP-Sepharose-purified GRK5 in the absence (Ctrl) or presence of the peptides listed in Table 1. Bsl (basal phosphorylation) refers to samples incubated with non-illuminated rhodopsin and in the absence of peptide. **A.** Peptides were used at 100 μM. Data shown are means ± SEM for at least three experiments performed in duplicate (*** $p < 0.001$, ** $p < 0.01$, * $p < 0.05$ by One-Way ANOVA). A representative autoradiogram is shown below the graph. **B.**

Molecular Pharmacology Fast Forward. Published on December 28, 2009 as DOI: 10.1124/mol.109.058115
This article has not been copyedited and formatted. The final version may differ from this version.

Peptides 1AA, 4, 6, and 7 were used at 10, 30, and 100 μM. Data shown are means ± SEM for three experiments performed in duplicate, except for peptide 4 (two experiments in duplicate at 10 and 30 μM). P values for peptides 1AA, 4, 6, and 7 at 30 μM were <0.01, <0.01, <0.001, and >0.05 respectively by One-Way ANOVA. **C.** Increasing concentrations of Rho* (0 – 25 μM) were incubated with purified 6His-GRK5 (4.6 nM) in the absence (Ctrl) or presence of peptide 6 (100 μM) for 10 min at 30 ºC. The experiment shown is representative of four similar experiments each performed in duplicate. Kinetic parameters for the control and peptide treated were as follows; V_{max} = 4.0 ± 1.1 and 1.0 ± 0.1 nmol/mg/min; and K_m = 11.7 ± 6.9 and 21.1 ± 4.0 μM respectively. An autoradiogram is shown below the graph. **D.** Peptides 4 and 6 (100μm) were incubated with Rho* (4μM) and either GRK5 (open bars) or GRK 6 (filled bars) for 10 min at 30 ºC. Data shown are the means ± SEM for three experiments performed in duplicate and normalized to % of control. A representative autoradiogram is shown below the graph.

Molecular Pharmacology Fast Forward. Published on December 28, 2009 as DOI: 10.1124/mol.109.058115
This article has not been copyedited and formatted. The final version may differ from this version.

Table 1. Sequences and modifications of the helix 9 peptides

Peptide	Sequence	Modification
1	E**F**DR**R**WR**QW**RE**L**WLR	Modified sequence except for ET residues, designed by PB[a]
1AA	Ac-E**F**DR**R**WR**QW**RE**L**WLR-NH_2	(AA) Acetylated and amidated peptide 1
2	D**F**EE**R**RR**QW**LI**L**YR	Modified sequence except for ET residues, designed by PB[a]
2AA	Ac-D**F**EE**R**RR**QW**LI**L**YR-NH_2	(AA) Acetylated and amidated peptide 2
3	EEY**F**KR**R**WE**QW**YK**L**Y	Modified sequence except for ET residues, designed by PB[a]
4	**Y**FN**R**FL**QW**KW**L**E	Unmodified GRK6 α9 (166-177)
5	Ac-**F**FD**R**FL**QW**KW**L**E-NH_2	Acetylated and amidated GRK5 α9 (166-177)
6	Ac-SNle**F**FD**R**FL**QW**KW**L**ER-NH_2	Acetylated and amidated GRK5 α9 (164-M165Nle-178)
7	Ac-SNle**F**FD**R**EL**QW**KW**L**ER-NH_2	E170 side chain – K174 side chain bridge
8	Ac-SNle**F**ED**R**FK**QW**KW**L**ER-NH_2	E167 side chain – K171 side chain bridge

[a] *PB: Peptide Builder*

ET residues are shown in bold and are underlined.

Peptides 6, 7, and 8: Nle was substituted for M165 to avoid sulfur oxidation.

Figure 1

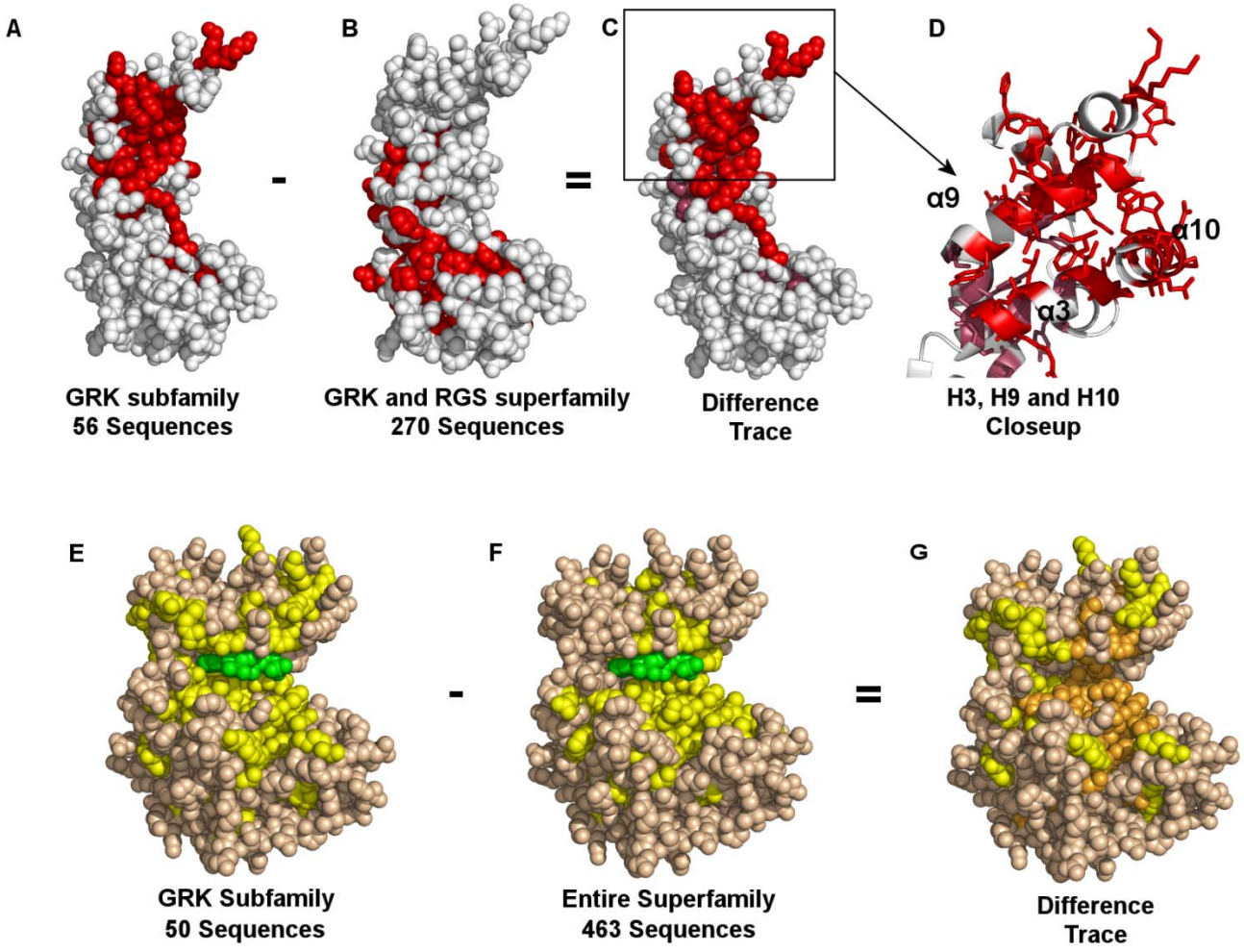

Figure 2

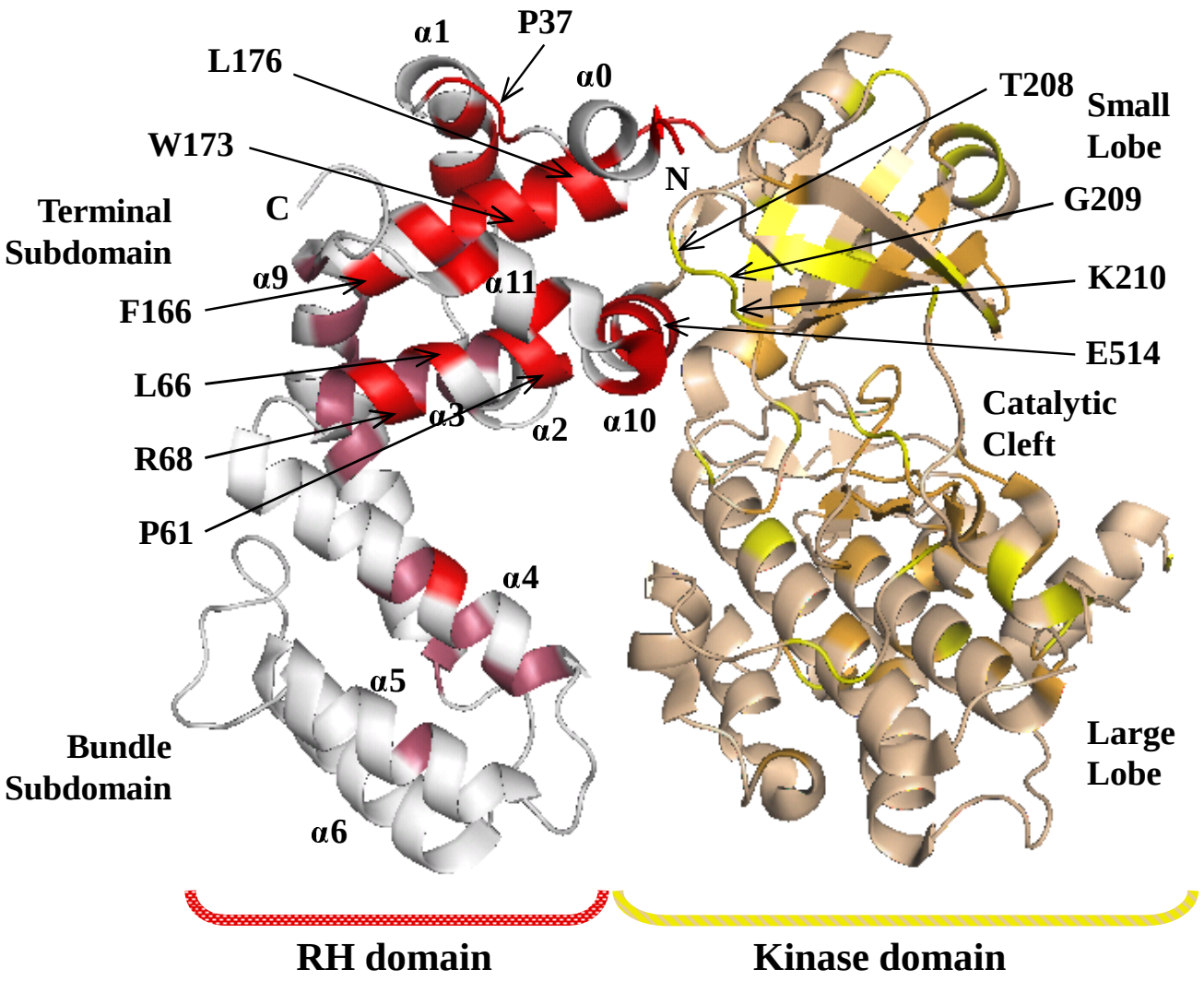

Figure 3

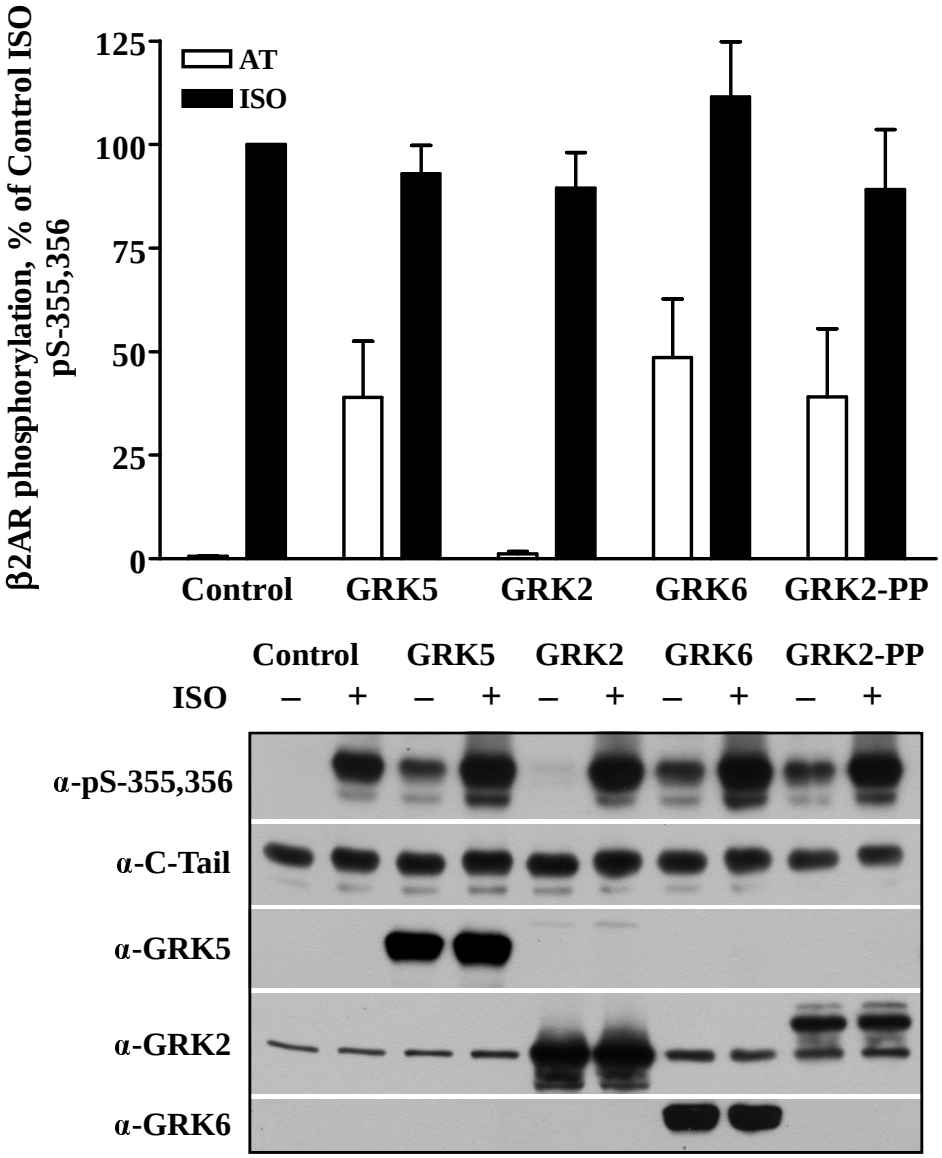

Figure 4

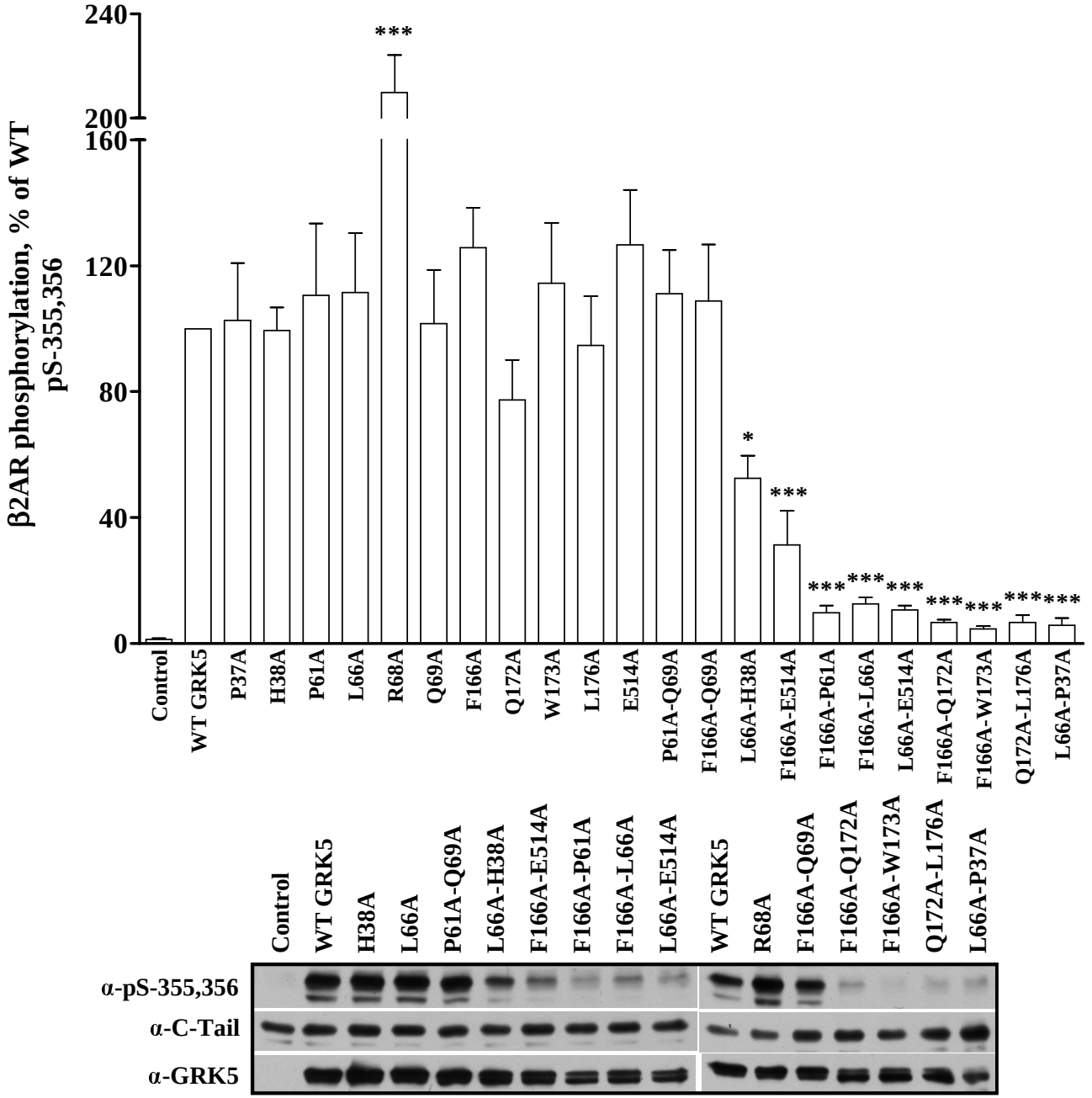

Molecular Pharmacology Fast Forward. Published on December 28, 2009 as DOI: 10.1124/mol.109.058115
This article has not been copyedited and formatted. The final version may differ from this version.

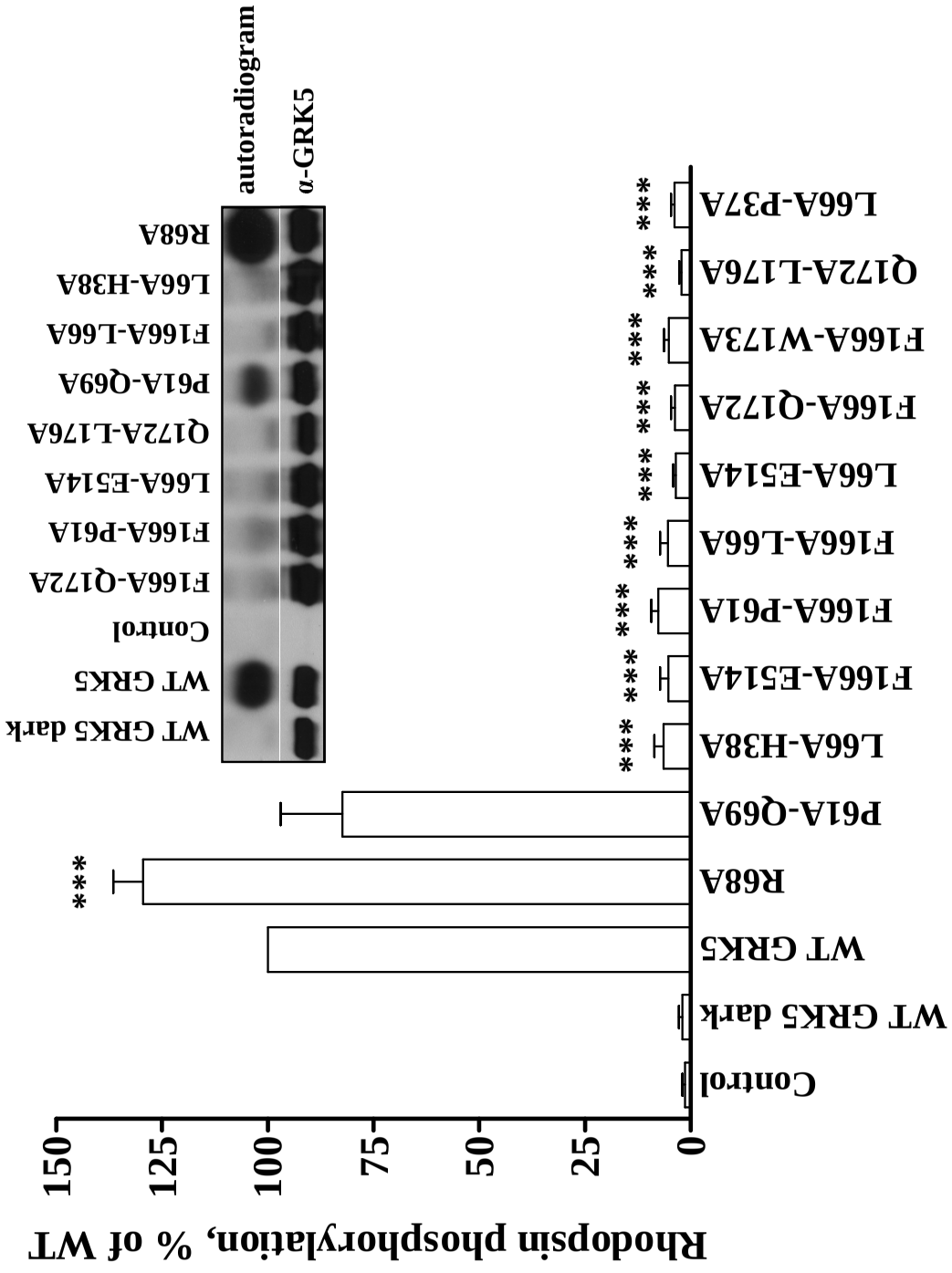

Figure 5

Figure 6

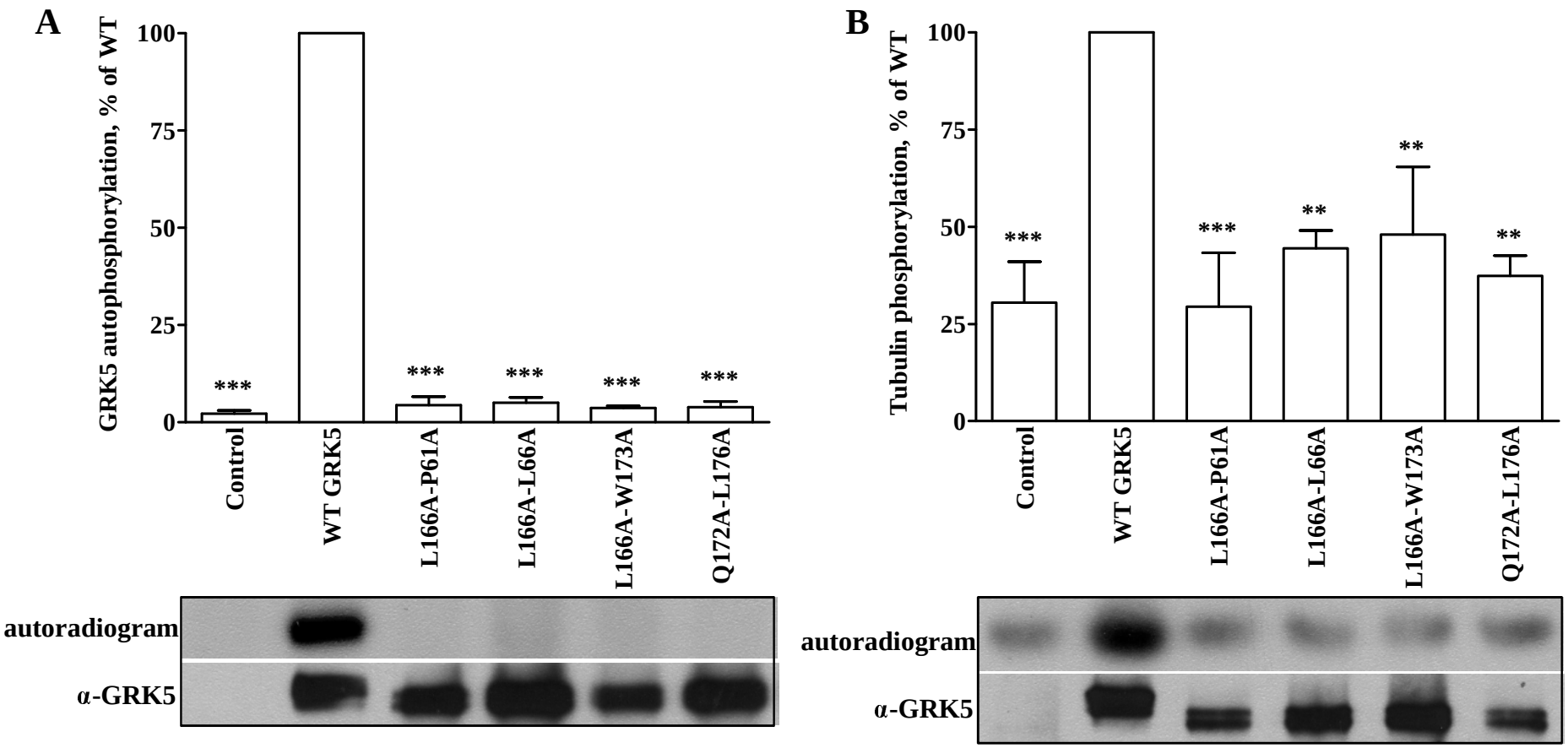

Figure 7

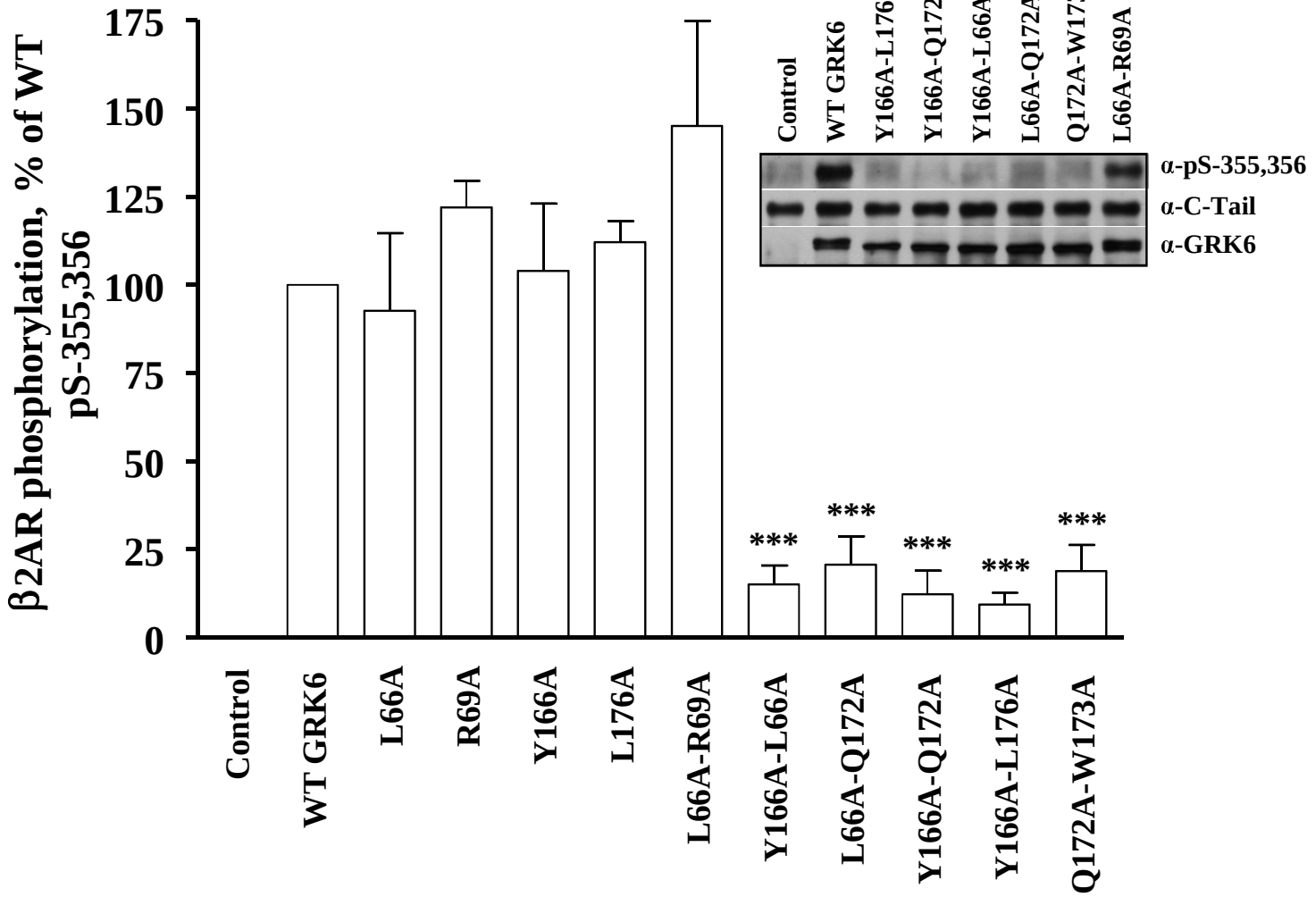

Molecular Pharmacology Fast Forward. Published on December 28, 2009 as DOI: 10.1124/mol.109.058115
This article has not been copyedited and formatted. The final version may differ from this version.

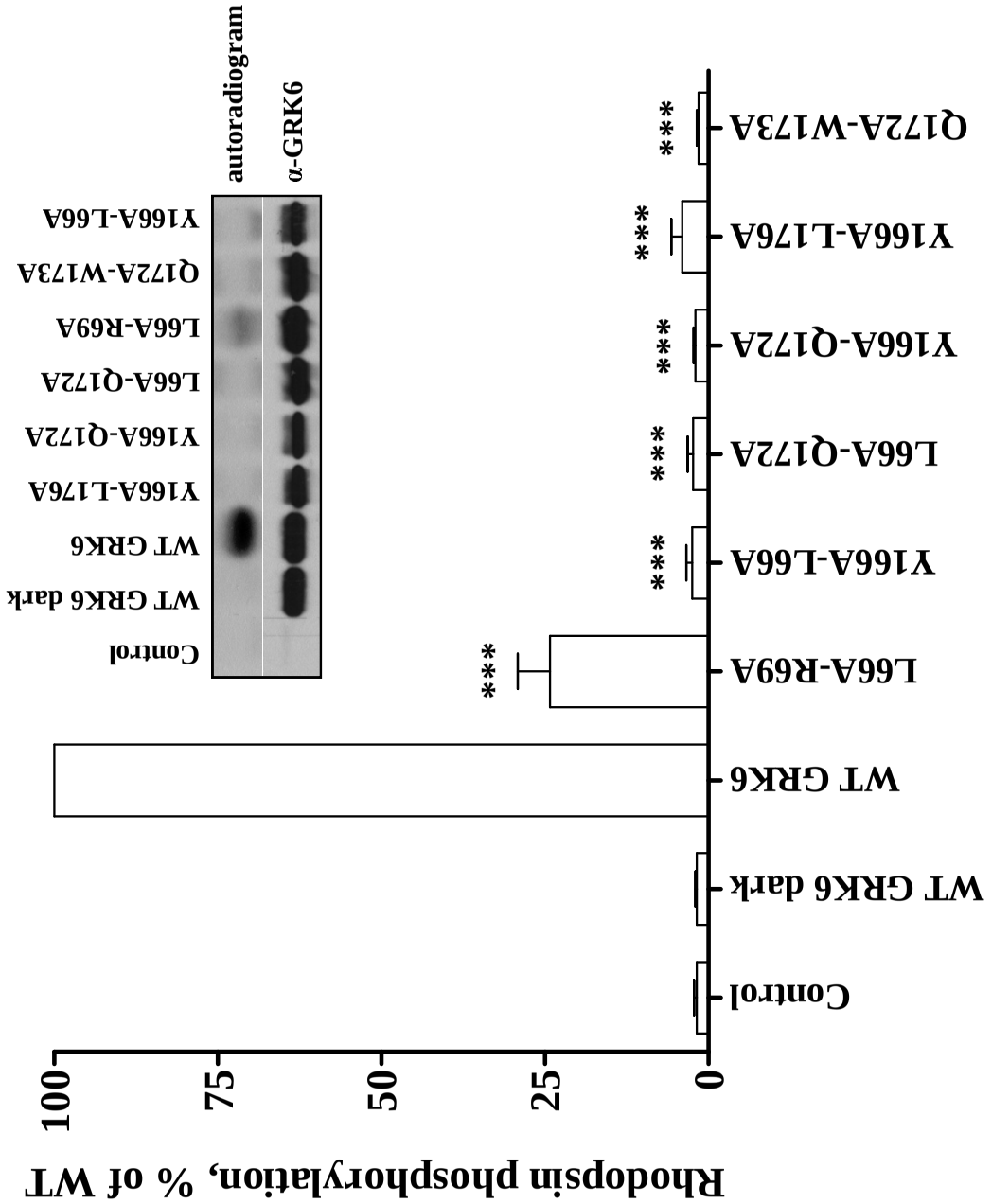

Figure 8

Figure 9